Usefulness of ultrasonic speckle decomposition procedure for tissue characterization

José Seabra, João Sanches *
Instituto de Sistemas e Robótica
Instituto Superior Técnico
Av. Rovisco Pais, 1049-001 Lisboa, Portugal
jseabra@isr.ist.utl.pt jmrs@ist.utl.pt

Abstract

Speckle is an inherent characteristic of tissues when assessed by ultrasound. De-speckling is performed to improve the visualization of anatomical details but the information encoded in speckle is often discarded. In this paper we propose an ultrasonic decomposition procedure which estimates de-speckled and speckle images starting with images created from Radio Frequency *(RF) data. These images are used to extract features of tissue echogenicity (acoustic properties) and textural information of the tissue parenchyma. Three-case studies demonstrate the usefulness of the proposed decomposition methodology for tissue characterization.*

1. Introduction

In the ultrasound image formation process a transmitted ultrasound pulse interacts with an anatomical region of interest providing information about internal tissue structures which is encoded in the backscatter echo. Moreover, an image features a characteristic granular pattern denoted in the literature by *speckle* [1]. Many statistical distributions have been proposed to model the envelope of ultrasound signals. In the case of *fully developed speckle* [3,9], the backscatter echo envelope can be described by a *Rayleigh* distribution, usually appropriated in (nearly) homogeneous tissue regions. The goal of the paper is to describe a complete and robust methodology providing useful echogenicity[1] and texture features for tissue characterization obtained from estimated de-speckled and speckle fields. Fig.1 displays a schematic diagram of the decomposition methodology, which consists of: (i) estimation of eRF image (image referring to the envelope of the RF data) from the *B-mode* image displayed by the ultrasound equipment, (ii) de-speckling estimation based on the *Rayleigh* distribution, performed in eRF images (either estimated or computed directly from available RF data), (iii) isolation of speckle field and (iv) tissue characterization.

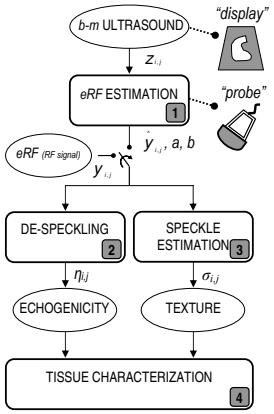

Figure 1. Architecture of the proposed decomposition procedure

2. De-speckling and Speckle estimation

Let $\mathbf{Y} = \{y_{i,j}\}$ be the estimated $N \times M$ eRF image. In this section we describe the procedure to estimate the de-speckled image $\mathbf{\Sigma} = \{\sigma_{i,j}\}$. Here, a Bayesian framework with the MAP criterion is adopted to deal with the ill poseness nature of the problem. Hence, the de-speckled image is obtained by minimizing an energy function,

$$\hat{\mathbf{\Sigma}} = \arg\min_{\mathbf{\Sigma}} E(\mathbf{Y}, \mathbf{\Sigma}), \tag{1}$$

where $E(\mathbf{Y}, \mathbf{\Sigma}) = E_d(\mathbf{Y}, \mathbf{\Sigma}) + E_p(\mathbf{\Sigma})$. $E_d(\mathbf{Y}, \mathbf{\Sigma})$, called *data fidelity* term, pushes the solution toward the data and $E_p(\mathbf{\Sigma})$, called *prior* term, regularizes the solution by introducing prior knowledge about $\mathbf{\Sigma}$. The *data fidelity* term is the *log-likelihood* function,$E_d(\mathbf{Y}, \mathbf{\Sigma}) = -\log(p(\mathbf{Y}|\mathbf{\Sigma}))$ where $p(\mathbf{Y}|\mathbf{\Sigma}) = \prod_{i,j=1}^{N,M} p(y_{i,j}|\sigma_{i,j})$ and $p(y_{i,j}|\sigma_{i,j}) = \frac{y_{i,j}}{\sigma_{i,j}^2} e^{-\frac{y_{i,j}^2}{2\sigma_{i,j}^2}}$ is the *Rayleigh* distribution [7]. The overall energy function, obtained after considering the variable change $x = \log(\sigma^2)$ is

*This work was supported by Fundação para a Ciência e a Tecnologia (ISR/IST plurianual funding) through the POS Conhecimento Program which includes FEDER funds.

[1] Echogenicity is the characteristic ability of a tissue to reflect sound waves and produce echoes.

given by:

$$E(\mathbf{Y},\mathbf{X}) = \sum_{i,j}\left[\frac{y_{i,j}^2}{2}e^{-x_{i,j}} + x_{i,j}\right] + \alpha TV(x_{i,j}) \qquad (2)$$

where $TV(x_{i,j}) = \sum_{i,j}\sqrt{(x_{i,j}-x_{i-1,j})^2 + (x_{i,j}-x_{i,j-1})^2}$. This energy function, where the *prior* term is the so called *Total Variation* (TV) of $\mathbf{X} = \{x_{i,j}\}$, is convex because all of its terms are convex (second derivative is positive). This means that its solution is unique and achievable.

The speckle corrupting the ultrasonic data is multiplicative in the sense that its variance depends on the underlying signal $\mathbf{\Sigma}$. The image formation model may be formulated as follows:

$$y_{i,j} = \eta_{i,j}\sigma_{i,j}, \qquad (3)$$

where $\sigma_{i,j}$ is the intensity of pixel (i,j) of the de-speckled image, while $y_{i,j}$ and $\eta_{i,j}$ are the corresponding pixel intensities in the eRF image and speckle field, respectively. The distribution of η is given by:

$$p(\eta_{i,j}) = \left|\frac{dy}{d\eta}\right| p(y) = \eta_{i,j}e^{-\eta_{i,j}^2/2}, \qquad \eta \geq 0, \qquad (4)$$

which is an unit parameter *Rayleigh* distribution independent of σ. The computation of the speckle field, $\mathbf{N} = \{\eta_{i,j}\}$, is performed from the estimated eRF image, $\mathbf{Y} = \{y_{i,j}\}$, and from the de-speckled one, $\mathbf{\Sigma} = \{\sigma_{i,j}\}$, yielding: $\eta_{i,j} = \frac{y_{i,j}}{\sigma_{i,j}}$.

3. Features extraction

In order to investigate the usefulness of the proposed methodology for tissue characterization, different types of features are extracted from the de-speckled and speckle images.

Echogenicity index The *echogenicity index*, referring to tissue distinct acoustic properties in a specific area, is represented by the averaged value $\bar{\sigma}^k$ of local echogenicity values $\sigma_{m,n}$ inside a block $k = \{\sigma_{m,n} : m = 1,...,M, n = 1,...,N\}$ extracted from the de-speckled image $\hat{\Sigma}$. This de-speckled image is used, for instance, in Fig. 2c.1.

Echogenicity decay The intensity decay along depth is a common phenomenon occurring in diffuse liver disease [4] and is also visible in high-reflectivity tissues, like calcified carotid and coronary plaques [6]. The feature referring to *echogenicity decay*, s_d, is obtained by linear regression over the mean values of each line of the block $k = \{\sigma_{m,n} : m = 1,...,M, n = 1,...,N\}$, $\bar{\sigma}_m^k = \sum_{n=1}^{N}\sigma_{m,n}$, where the cost function to be minimized is given by:

$$J = \sum_{m=1}^{M}(s_d\, m + b - \bar{\sigma}_m^k)^2. \qquad (5)$$

Figs. 2b.1-b.2 illustrate the distinct intensity profiles in de-speckled images for normal and pathologic liver, overlayed with the estimated *echogenicity decays* for each case.

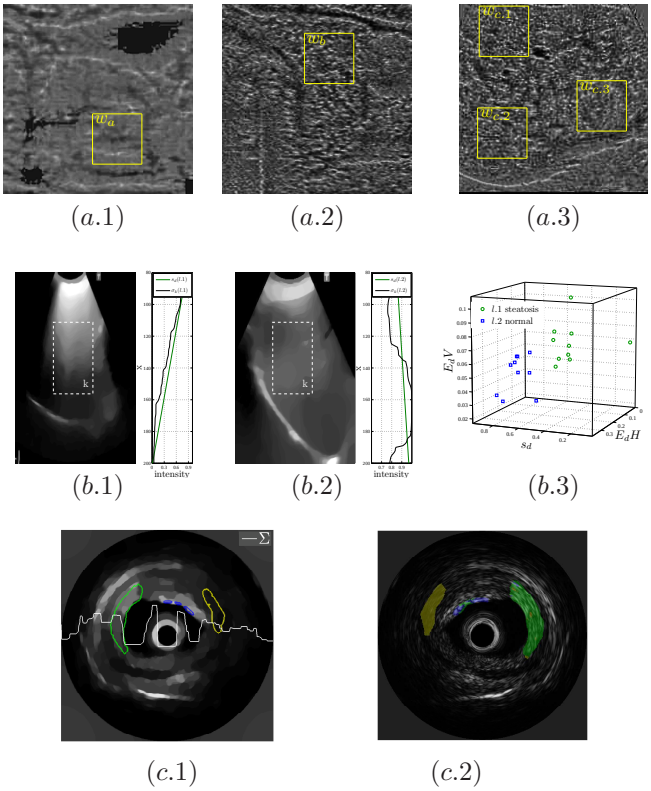

Figure 2. Case Studies

Speckle-derived wavelet energies The structure and directionality of speckle is hypothesized as being a relevant feature for tissue discrimination. Thus, suitable textural descriptors could be extracted from the isolated speckle field by considering the first Haar wavelet decomposition energies, particularly the approximation energy E_a, together with horizontal E_dH and vertical detail energies E_dV. Additionally, to quantify the relative detail in each direction, the ratio of horizontal to vertical detail energies, $r_{HV} = \frac{E_dH}{E_dV}$ is computed, where $r_{HV} \approx 1$ means that there is no predominant speckle directionality.

4. Results

In summary, the de-speckling process produces a de-speckled image, carrying information about the local tissue echogenicity, and a speckle field, related to the structure and the characteristic pattern of a local tissue area. It becomes now important to demonstrate that the estimated outcomes of the overall decomposition procedure, specifically the de-speckled image and speckle field, provide information that is properly related to different morphological and textural properties of the tissue. Given this, we present 3 case studies using distinct ultrasonic data, which are here described (Fig. 2 and Table 1).

	Description	Features	Results	Observations
$C.S.1$	inter and intra- tissue textural analysis from computed speckle fields of carotid plaque, thyroid and liver (Fig. 2a)	wavelet based detail energies	w_a: E_a=99.57 E_d=0.43 r_{HV}=2.8 w_b: E_a=95.43 E_d=4.57 r_{HV}=4.7 $w_c.1$: E_a=92.34 E_d=7.66 r_{HV}=2.3 $w_c.2$: E_a=94.32 E_d=5.68 r_{HV}=3.1 $w_c.3$: E_a=96.30 E_d=3.70 r_{HV}=2.1	features differ significantly from one anatomical structure to another, as well as from one tissue area to another
$C.S.2$	liver steatosis binary classification (Fig. 2b) [5], using a sample of 20 livers, clinically labelled as normal or steatotic (with abnormal lipid retention)	wavelet based detail energies; *echogenicity decay* from de-speckled image (Figs.2b.1-b.2)	Sensitivity: S=1.00 Specificity: K=0.95 $l.1$: $\bar{s}_d$=0.48 (0.18) $\bar{E}_dH$=9.79 (2.68) $\bar{E}_dV$=6.78 (1.63) $l.2$: $\bar{s}_d$=0.80 (0.11) $\bar{E}_dH$=19.97 (4.54) $\bar{E}_dV$=4.66 (1.61)	High sensitity and specificity results Good discrimination between classes (normal vs. steatotic livers) in Fig.2b.3
$C.S.3$	IVUS 3-type plaque tissue classification [2] using 67 plaques labelled as fibrotic, lipidic and calcified (Fig. 2c)	*echogenicity index* from de-speckled image	Accuracy: A= $91.37(5.02$ Sensitivities: S_{fib}=0.91 (0.05) S_{lip}=0.94 (0.04) S_{cal}=0.91 (0.05)	the inclusion of speckle features improves the classification performance obtained with an already existing classification framework [2]
$C.S.3$	subject identification based on thyroid tissue [8], considering a population of 10 subjects (several samples per subject)	wavelet decomposition based detail energies obtained from speckle; *echogenicity index* from de-speckled image	Sensitivities: $S(f.1)$=0.79 (0.15) $S(f.2)$=0.70 (0.07) $S(f.1,2)$=0.94 (0.10)	High sensitity values, specially when features are combined

Table 1. Summary table

5. Conclusions

In this paper, a decomposition procedure is proposed which is able to estimate the de-speckled and speckle components of an ultrasound image, providing additional sources of information, referring to echogenicity and texture. The inclusion of this information in distinct studies here presented showed to be favorable for tissue characterization.

References

[1] C. Burckhardt. Speckle in ultrasound B-mode scans. *IEEE Transations on Sonics and Ultrasonics*, SU-25(1):1–6, 1978.

[2] F. Ciompi. Ecoc-based plaque classification using in-vivo and ex-vivo intravascular ultrasound data. *Master thesis*, 2008.

[3] T. Eltoft. Modeling the amplitude statistics of ultrasonic images. *IEEE Transactions on Medical Imaging*, 25(2):229–240, Feb 2006. Comparative Study.

[4] C. Lee, J. Choi, K. Kim, T. Seo, J. Lee, and C. Park. Usefulness of standard deviation on the histogram of ultrasound as a quantitative value for hepatic parenchymal echo texture; preliminary study. *Ultrasound Med Biol*, 32(12):1817–26, 2006.

[5] R. Ribeiro and J. Sanches. Fatty liver characterization and classification by ultrasound. In *IbPRIA '09: Proceedings of the 4th Iberian Conference on Pattern Recognition and Image Analysis*, pages 354–361, Berlin, Heidelberg, 2009. Springer-Verlag.

[6] Y. Saijo, A. Tanaka, H. Sasaki, T. Iwamoto, E. S. Filho, M. Yoshizawa, and T. Yambe. Basic ultrasonic characteristics of atherosclerosis measured by intravascular ultrasound and acoustic microscopy. *International Congress Series*, 1274:116 – 121, 2004.

[7] J. M. Sanches, J. C. Nascimento, and J. S. Marques. Medical image noise reduction using the sylvester-lyapunov equation. *IEEE Transactions on Image Processing*, 17(9):1522–1539, 2008.

[8] J. Seabra and A. Fred. Towards the development of a thyroid ultrasound biometric scheme based on tissue echo-morphological features. In *Communications in Computer and Information Science*. Springer-Verlag, 2009. (to appear).

[9] R. F. Wagner, S. W. Smith, J. M. Sandrik, and H. Lopez. Statistics of speckle in ultrasound b-scans. *Sonics and Ultrasonics, IEEE Transactions on*, 30(3):156–163, 1983.